

12

Discrete & Continuous Nonlinear Dynamics

Nonlinear dynamics is one of the success stories of computational science. It has been explored by mathematicians, scientists, and engineers, with computers as an essential tool. The computations have led to the discovery of new phenomena such as solitons, chaos, and fractals, as you will discover on your own. In addition, because biological systems often have complex interactions and may not be in thermodynamic equilibrium states, models of them are often nonlinear, with properties similar to those of other complex systems.

In Unit I we develop the logistic map as a model for how bug populations achieve dynamic equilibrium. It is an example of a very simple but nonlinear equation producing surprising complex behavior. In Unit II we explore chaos for a continuous system, the driven realistic pendulum. Our emphasis there is on using phase space as an example of the usefulness of an abstract space to display the simplicity underlying complex behavior. In Unit III we extend the discrete logistic map to nonlinear differential models of coupled predator–prey populations and their corresponding phase space plots.

12.1 Unit I. Bug Population Dynamics (Discrete)

Problem: The populations of insects and the patterns of weather do not appear to follow any simple laws.¹ At times they appear stable, at other times they vary periodically, and at other times they appear chaotic, only to settle down to something simple again. Your **problem** is to deduce if a simple, discrete law can produce such complicated behavior.

12.2 The Logistic Map (Model)

Imagine a bunch of insects reproducing generation after generation. We start with N_0 bugs, then in the next generation we have to live with N_1 of them, and after i generations there are N_i bugs to bug us. We want to define a model of how N_n varies with the discrete generation number n . For guidance, we look to the radioactive decay simulation in Chapter 5, “Monte Carlo Simulations”, where the

¹ Except maybe in Oregon, where storm clouds come to spend their weekends.



COPYRIGHT 2008, PRINCETON UNIVERSITY PRESS

EVALUATION COPY ONLY. NOT FOR USE IN COURSES.

discrete decay law, $\Delta N/\Delta t = -\lambda N$, led to exponential-like decay. Likewise, if we reverse the sign of λ , we should get exponential-like growth, which is a good place to start our modelling. We assume that the bug-breeding rate is proportional to the number of bugs:

$$\frac{\Delta N_i}{\Delta t} = \lambda N_i. \quad (12.1)$$

Because we know as an empirical fact that exponential growth usually tapers off, we improve the model by incorporating the observation that bugs do not live on love alone; they must also eat. But bugs, not being farmers, must compete for the available food supply, and this might limit their number to a maximum N_* (called the *carrying capacity*). Consequently, we modify the exponential growth model (12.1) by introducing a growth rate λ' that decreases as the population N_i approaches N_* :

$$\lambda = \lambda'(N_* - N_i) \Rightarrow \frac{\Delta N_i}{\Delta t} = \lambda'(N_* - N_i)N_i. \quad (12.2)$$

We expect that when N_i is small compared to N_* , the population will grow exponentially, but that as N_i approaches N_* , the growth rate will decrease, eventually becoming negative if N_i exceeds N_* , the carrying capacity.

Equation (12.2) is one form of the *logistic map*. It is usually written as a relation between the number of bugs in future and present generations:

$$N_{i+1} = N_i + \lambda' \Delta t (N_* - N_i) N_i, \quad (12.3)$$

$$= N_i (1 + \lambda' \Delta t N_*) \left[1 - \frac{\lambda' \Delta t}{1 + \lambda' \Delta t N_*} N_i \right]. \quad (12.4)$$

The map looks simple when expressed in terms of natural variables:

$$x_{i+1} = \mu x_i (1 - x_i), \quad (12.5)$$

$$\mu \stackrel{\text{def}}{=} 1 + \lambda' \Delta t N_*, \quad x_i \stackrel{\text{def}}{=} \frac{\lambda' \Delta t}{\mu} N_i \simeq \frac{N_i}{N_*}, \quad (12.6)$$

where μ is a dimensionless growth parameter and x_i is a dimensionless population variable. Observe that the *growth rate* μ equals 1 when the breeding rate λ' equals 0, and is otherwise expected to be larger than 1. If the number of bugs born per generation $\lambda' \Delta t$ is large, then $\mu \simeq \lambda' \Delta t N_*$ and $x_i \simeq N_i/N_*$. That is, x_i is essentially a fraction of the carrying capacity N_* . Consequently, we consider x values in the range $0 \leq x_i \leq 1$, where $x = 0$ corresponds to no bugs and $x = 1$ to the maximum population. Note that there is clearly a linear, quadratic dependence of the RHS of (12.5) on x_i . In general, a map uses a function $f(x)$ to map one number in a



sequence to another,

$$x_{i+1} = f(x_i). \quad (12.7)$$

For the logistic map, $f(x) = \mu x(1 - x)$, with the quadratic dependence of f on x making this a nonlinear map, while the dependence on only the one variable x_i makes it a *one-dimensional* map.

12.3 Properties of Nonlinear Maps (Theory)

Rather than do some fancy mathematical analysis to determine the properties of the logistic map [Rash 90], we prefer to have you study it directly on the computer by plotting x_i *versus* generation number i . Some typical behaviors are shown in Figure 12.1. In Figure 12.1A we see equilibration into a single population; in Figure 12.1B we see oscillation between two population levels; in Figure 12.1C we see oscillation among four levels; and in Figure 12.1D we see a chaotic system. The initial population x_0 is known as the *seed*, and as long as it is not equal to zero, its exact value usually has little effect on the population dynamics (similar to what we found when generating pseudorandom numbers). In contrast, the dynamics are unusually sensitive to the value of the growth parameter μ . For those values of μ at which the dynamics are complex, there may be extreme sensitivity to the initial condition x_0 as well as to the exact value of μ .

12.3.1 Fixed Points

An important property of the map (12.5) is the possibility of the sequence x_i reaching a *fixed* point at which x_i remains or fluctuates about. We denote such fixed points as x_* . At a *one-cycle* fixed point, there is no change in the population from generation i to generation $i + 1$; that is,

$$x_{i+1} = x_i = x_*. \quad (12.8)$$

Using the logistic map (12.5) to relate x_{i+1} to x_i yields the algebraic equation

$$\mu x_*(1 - x_*) = x_* \Rightarrow x_* = 0 \quad \text{or} \quad x_* = \frac{\mu - 1}{\mu}. \quad (12.9)$$

The nonzero fixed point $x_* = (\mu - 1)/\mu$ corresponds to a stable population with a balance between birth and death that is reached regardless of the initial population (Figure 12.1A). In contrast, the $x_* = 0$ point is unstable and the population remains static only as long as no bugs exist; if even a few bugs are introduced, exponential growth occurs. Further analysis (§12.8) tells us that the stability of a population is determined by the magnitude of the derivative of the mapping function $f(x_i)$ at

— -1
— 0
— 1



COPYRIGHT 2008, PRINCETON UNIVERSITY PRESS

EVALUATION COPY ONLY. NOT FOR USE IN COURSES.

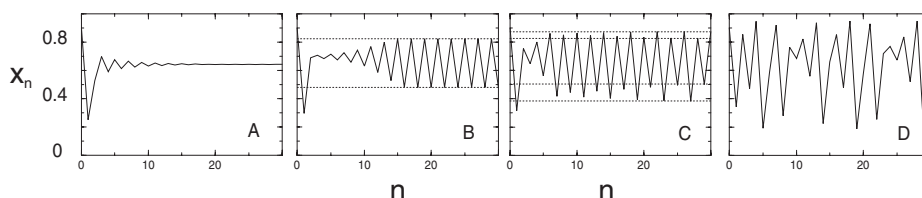


Figure 12.1 The insect population x_n versus the generation number n for various growth rates. (A) $\mu = 2.8$, a period-one cycle. If the fixed point is $x_n = 0$, the system becomes extinct. (B) $\mu = 3.3$, a period-two cycle. (C) $\mu = 3.5$, a period-four cycle. (D) $\mu = 3.8$, a chaotic regime. If $\mu < 1$, the population goes extinct.

the fixed point [Rash 90]:

$$\left| \frac{df}{dx} \right|_{x_*} < 1 \quad (\text{stable}). \quad (12.10)$$

For the one cycle of the logistic map (12.5), we have

$$\left. \frac{df}{dx} \right|_{x_*} = \mu - 2\mu x_* = \begin{cases} \mu, & \text{stable at } x_* = 0 \text{ if } \mu < 1, \\ 2 - \mu, & \text{stable at } x_* = \frac{\mu-1}{\mu} \text{ if } \mu < 3. \end{cases} \quad (12.11)$$

12.3.2 Period Doubling, Attractors

Equation (12.11) tells us that while the equation for fixed points (12.9) may be satisfied for all values of μ , the populations will not be stable if $\mu > 3$. For $\mu > 3$, the system's long-term population *bifurcates* into two populations (a *two-cycle*), an effect known as *period doubling* (Figure 12.1B). Because the system now acts as if it were attracted to two populations, these populations are called *attractors* or *cycle points*. We can easily predict the x values for these two-cycle attractors by demanding that generation $i + 2$ have the same population as generation i :

$$x_i = x_{i+2} = \mu x_{i+1}(1 - x_{i+1}) \Rightarrow x_* = \frac{1 + \mu \pm \sqrt{\mu^2 - 2\mu - 3}}{2\mu}. \quad (12.12)$$

We see that as long as $\mu > 3$, the square root produces a real number and thus that physical solutions exist (complex or negative x_* values are nonphysical). We leave it to your computer explorations to discover how the system continues to double periods as μ continues to increase. In all cases the pattern is the same: One of the populations bifurcates into two.



COPYRIGHT 2008, PRINCETON UNIVERSITY PRESS

EVALUATION COPY ONLY. NOT FOR USE IN COURSES.

Program the logistic map to produce a sequence of population values x_i as a function of the generation number i . These are called *map orbits*. The assessment consists of confirmation of Feigenbaum's observations [Feig 79] of the different behavior patterns shown in Figure 12.1. These occur for growth parameter $\mu = (0.4, 2.4, 3.2, 3.6, 3.8304)$ and seed population $x_0 = 0.75$. Identify the following on your graphs:

- The system's behavior in the chaotic region is critically dependent on the exact values of μ and x_0 . Systems may start out with nearly identical values for μ and x_0 but end up with quite different ones. In some cases the complicated behaviors of nonlinear systems will be *chaotic*, but unless you have a bug in your program, they will not be random.²

- ²You may recall from Chapter 5, “Monte Carlo Simulations,” that a random sequence of events does not even have step-by-step correlations.

EVALUATION COPY ONLY. NOT FOR USE IN COURSES.

- b. Repeat the simulation with $x_0 = 0.75$ and two essentially identical survival parameters, $\mu = 4.0$ and $\mu' = 4.0(1 - \epsilon)$. Both simulations should start off the same but eventually diverge. |

12.5 Bifurcation Diagram (Assessment)

Computing and watching the population change with generation number gives a good idea of the basic dynamics, at least until it gets too complicated to discern patterns. In particular, as the number of bifurcations keeps increasing and the system becomes chaotic, it is hard for us to see a simple underlying structure within the complicated behavior. One way to visualize what is going on is to concentrate on the attractors, that is, those populations that appear to attract the solutions and to which the solutions continuously return. A plot of these attractors (long-term iterates) of the logistic map as a function of the growth parameter μ is an elegant way to summarize the results of extensive computer simulations.

A *bifurcation diagram* for the logistic map is given in Figure 12.2, while one for a Gaussian map is given in Figure 12.3. For each value of μ , hundreds of iterations are made to make sure that all transients essentially die out, and then the values (μ, x_*) are written to a file for hundreds of iterations after that. If the system falls into an n cycle for this μ value, then there should predominantly be n different values written to the file. Next, the value of the initial populations x_0 is changed slightly, and the entire procedure is repeated to ensure that no fixed points are missed. When finished, your program will have stepped through all the values of growth parameter μ , and for each value of μ it will have stepped through all the values of the initial population x_0 . Our sample program Bugs.java is shown in Listing 12.1.

```
// Bugs.java: Bifurcation diagram for logistic map
import java.io.*;

public class Bugs {
    static double m_min = 0.0, m_max = 4., step = 0.01 ;           // Class variables

    public static void main(String[] argv) throws IOException, FileNotFoundException {
        double m, y;
        int i;
        PrintWriter w = new PrintWriter(new FileOutputStream("Bugs.dat"), true);
        for ( m = m_min; m <= m_max; m += step ) {                 // mu loop
            y = 0.5;                                                // Arbitrary seed
            for ( i=1; i <=200; i++ ) y = m*y*(1-y);                // Transients
            for ( i=201; i <=401; i++ ) {
                y = m*y*(1-y);
                w.println( " "+ m+" "+ y);
            }
            System.out.println("sorted data stored in Bugs.dat.");
        }
    }
}
```

Listing 12.1 Bugs.java, the basis of a program for producing the bifurcation diagram of the logistic map. A finished program requires finer grids, a scan over initial values, and removal of duplicates.

— 1
— 0
— 1



COPYRIGHT 2008, PRINCETON UNIVERSITY PRESS

EVALUATION COPY ONLY. NOT FOR USE IN COURSES.

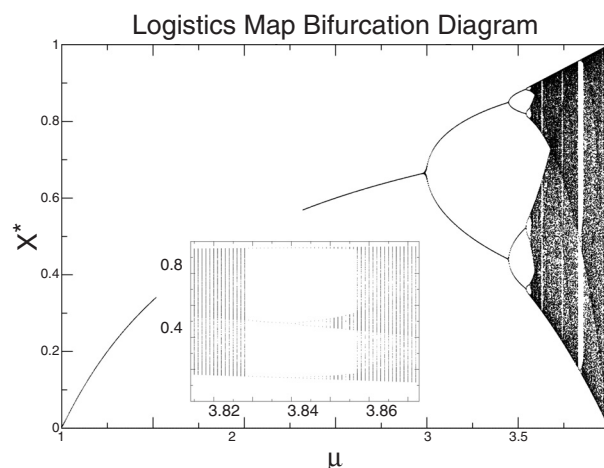


Figure 12.2 The bifurcation plot, attractor populations *versus* growth rate, for the logistic map. The inset shows some details of a three-cycle window.

12.5.1 Bifurcation Diagram Implementation

The last part of this problem is to reproduce Figure 12.2 at various levels of detail. (You can listen to a sonification of this diagram on the CD or use one of the applet there to create your own sonification.) While the best way to make a visualization of this sort would be with visualization software that permits you to vary the intensity of each individual point on the screen, we simply plot individual points and have the density in each region determined by the number of points plotted there. When thinking about plotting many individual points to draw a figure, it is important to keep in mind that your screen resolution is ~ 100 dots per inch and your laser printer resolution may be 300 dots per inch. This means that if you plot a point at each pixel, you will be plotting $\sim 3000 \times 3000 \approx 10$ million elements. *Beware:* This can require some time and may choke a printer. In any case, printing at a finer resolution is a waste of time.



12.5.2 Visualization Algorithm: Binning

1. Break up the range $1 \leq \mu \leq 4$ into 1000 steps and loop through them. These are the “bins” into which we will place the x_* values.
2. In order not to miss any structures in your bifurcation diagram, loop through a range of initial x_0 values as well.
3. Wait at least 200 generations for the transients to die out and then print the next several hundred values of (μ, x_*) to a file.

— -1
— 0
— 1



COPYRIGHT 2008, PRINCETON UNIVERSITY PRESS

EVALUATION COPY ONLY. NOT FOR USE IN COURSES.

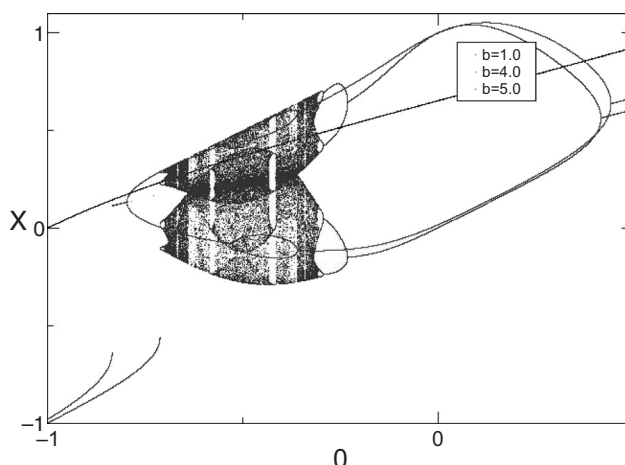


Figure 12.3 A bifurcation plot for the Gaussian map. (Courtesy of W. Hager.)

4. Print your x_* values to no more than three or four decimal places. You will not be able to resolve more places than this on your plot, and this restriction will keep your output files smaller by permitting you to remove duplicates. It is hard to control the number of decimal places in the output with Java's standard print commands (although `printf` and `DecimalFormat` do permit control). A simple approach is to multiply the x_i values by 1000 and then throw away the part to the right of the decimal point. Because $0 \leq x_n \leq 1$, this means that $0 \leq 100 * x_n \leq 1000$, and you can throw away the decimal part by casting the resulting numbers as integers:

```
ix[i]=(int)(1000*x[i])                                // Convert to  $0 \leq \text{ints} \leq 1000$ 
```

You may then divide by 1000 if you want floating-point numbers.

5. You also need to remove duplicate values of (x, μ) from your file (they just take up space and plot on top of each other). You can do that in Unix/Linux with the `sort -u` command.
6. Plot your file of x_* versus μ . Use small symbols for the points and do not connect them.
7. Enlarge sections of your plot and notice that a similar bifurcation diagram tends to be contained within each magnified portion (this is called *self-similarity*).
8. Look over the series of bifurcations occurring at

$$\mu_k \simeq 3, 3.449, 3.544, 3.5644, 3.5688, 3.569692, 3.56989, \dots \quad (12.13)$$

The end of this series is a region of chaotic behavior.



COPYRIGHT 2008, PRINCETON UNIVERSITY PRESS

EVALUATION COPY ONLY. NOT FOR USE IN COURSES.

9. Inspect the way this and other sequences begin and then end in chaos. The changes sometimes occur quickly, and so you may have to make plots over a very small range of μ values to see the structures.
10. A close examination of Figure 12.2 shows regions where, with a slight increase in μ , a very large number of populations suddenly change to very few populations. Whereas these may appear to be artifacts of the video display, this is a real effect and these regions are called *windows*. Check that at $\mu = 3.828427$, chaos turns into a three-cycle population. ■

12.5.3 Feigenbaum Constants (Exploration)

Feigenbaum discovered that the sequence of μ_k values (12.13) at which bifurcations occur follows a regular pattern [Feig 79]. Specifically, it converges geometrically when expressed in terms of the distance between bifurcations δ :

$$\mu_k \rightarrow \mu_\infty - \frac{c}{\delta^k}, \quad \delta = \lim_{k \rightarrow \infty} \frac{\mu_k - \mu_{k-1}}{\mu_{k+1} - \mu_k}. \quad (12.14)$$

Use your sequence of μ_k values to determine the constants in (12.14) and compare them to those found by Feigenbaum:

$$\mu_\infty \simeq 3.56995, \quad c \simeq 2.637, \quad \delta \simeq 4.6692. \quad (12.15)$$

Amazingly, the value of the *Feigenbaum constant* δ is universal for all second-order maps.

12.6 Random Numbers via Logistic Map (Exploration) ⊙

There are claims that the logistic map in the chaotic region ($\mu \geq 4$),

$$x_{i+1} \simeq 4x_i(1 - x_i), \quad (12.16)$$

can be used to generate random numbers [P&R 95]. Although successive x_i 's are correlated, if the population for approximately every sixth generation is examined, the correlation is effectively gone and random numbers result. To make the sequence more uniform, a trigonometric transformation is used:

$$y_i = \frac{1}{\pi} \cos^{-1}(1 - 2x_i). \quad (12.17)$$

Use the random-number tests discussed in Chapter 5, "Monte Carlo Simulation," to test this claim.

— 1
— 0
— 1



COPYRIGHT 2008, PRINCETON UNIVERSITY PRESS

EVALUATION COPY ONLY. NOT FOR USE IN COURSES.

TABLE 12.1
Several Nonlinear Maps to Explore

Name	$f(x)$	Name	$f(x)$
Logistic	$\mu x(1-x)$	Tent	$\mu(1-2 x-1/2)$
Ecology	$xe^{\mu(1-x)}$	Quartic	$\mu[1-(2x-1)^4]$
Gaussian	$e^{bx^2} + \mu$		

12.7 Other Maps (Exploration)

Bifurcations and chaos are characteristic properties of nonlinear systems. Yet systems can be nonlinear in a number of ways. Table 12.1 lists four maps that generate x_i sequences containing bifurcations. The tent map derives its nonlinear dependence from the absolute value operator, while the logistic map is a subclass of the ecology map. Explore the properties of these other maps and note the similarities and differences.

12.8 Signals of Chaos: Lyapunov Coefficients ◉

The Lyapunov coefficient λ_i provides an analytic measure of whether a system is chaotic [Wolf 85, Ram 00, Will 97]. Physically, the coefficient is a measure of the growth rate of the solution near an attractor. For 1-D maps there is only one such coefficient, whereas in general there is a coefficient for each direction in space. The essential assumption is that neighboring paths x_n near an attractor have an n (or time) dependence $L \propto \exp(\lambda t)$. Consequently, orbits that have $\lambda > 0$ diverge and are chaotic; orbits that have $\lambda = 0$ remain marginally stable, while orbits with $\lambda < 0$ are periodic and stable. Mathematically, the Lyapunov coefficient or exponent is defined as

$$\lambda = \lim_{t \rightarrow \infty} \frac{1}{t} \log \frac{L(t)}{L(t_0)}, \quad (12.18)$$

where $L(t)$ is the distance between neighboring phase space trajectories at time t .

We calculate the Lyapunov exponent for a general 1-D map,

$$x_{n+1} = f(x_n), \quad (12.19)$$

and then apply the result to the logistic map. To determine stability, we examine perturbations about a reference trajectory x_0 by adding a small perturbation and iterating once [Mann 90, Ram 00]:

$$\hat{x}_0 = x_0 + \delta x_0, \quad \hat{x}_1 = x_1 + \delta x_1. \quad (12.20)$$



COPYRIGHT 2008, PRINCETON UNIVERSITY PRESS

EVALUATION COPY ONLY. NOT FOR USE IN COURSES.

$$\begin{aligned} x_1 + \delta x_1 &= f(x_0 + \delta x_0) \simeq f(x_0) + \left. \frac{\delta f}{\delta x} \right|_{x_0} \delta x_0 = x_1 + \left. \frac{\delta f}{\delta x} \right|_{x_0} \delta x_0, \\ \Rightarrow \quad \delta x_1 &\simeq \left(\left. \frac{\delta f}{\delta x} \right|_{x_0} \right) \delta x_0. \end{aligned} \quad (12.21)$$
$$\delta x_2 \simeq \left(\frac{\delta f}{\delta x} \right)_{x_1} \delta x_1 = \left(\frac{\delta f}{\delta x} \right)_{x_0} \left(\frac{\delta f}{\delta x} \right)_{x_1} \delta x_0, \quad (12.22)$$

$$|\delta x_n| = L^n |\delta x_0|, \quad L^n = \prod_{i=0}^{n-1} \left| \left(\frac{\delta f}{\delta x} \right)_{x_i} \right|. \quad (12.24)$$

$$\lambda = \ln(L) = \lim_{n \rightarrow \infty} \frac{1}{n} \sum_{i=0}^{n-1} \ln \left| \left(\frac{\delta f}{\delta x} \right)_{x_i} \right|. \quad (12.25)$$
$$\lambda = \frac{1}{n} \sum_{i=0}^{n-1} \ln |\mu - 2\mu x_i|, \quad (12.26)$$

The code `LyapLog.java` in Listing 12.2 computes the Lyapunov exponents for the bifurcation plot of the logistic map. In Figure 12.4 left we show its output and note the sign changes in λ where the system becomes chaotic, and abrupt changes in slope at bifurcations. (A similar curve is obtained for the fractal dimension of the logistic map, as indeed the two are proportional.)

Shannon entropy, like the Lyapunov exponent, is another analytic measure of chaos. It is a measure of uncertainty that has proven useful in communication theory

```
// LyapLog.java: Lyapunov coef for logistic map
import java.io.*;

public class LyapLog {
    static double m_min = 2.8, m_max = 4., step = 0.002 ;

    public static void main(String[] argv) throws IOException, FileNotFoundException {
        double m, y, suma, lyap[] = new double[100];
        int i;
        PrintWriter w = new PrintWriter(new FileOutputStream("logistic.dat"), true);
        PrintWriter q = new PrintWriter(new FileOutputStream("lyap.dat"), true);
        System.out.println("data stored in logistic.dat and lyap.dat");
        for ( m = m_min; m <= m_max; m += step ) { // m loop
            y = 0.5;
            for ( i=1; i <= 200; i++ ) y = m*y*(1-y);
            suma = 0.; // Skip transients
            for ( i=201; i <= 401; i++ ) {
                y = m*y*(1-y);
                suma = suma + Math.log(Math.abs(m*(1.-2.*y))); // Lyapunov
                w.println( m + " " + y );
            }
            lyap[(int)m] = suma/401; // Normalize Lyapunov exponent
            q.println( m + " " + lyap[(int)m] );
        } }
}
```

Listing 12.2 `LyapLog.java` computes Lyapunov exponents for the bifurcation plot of the logistic map as a function of growth rate. Note the fineness of the μ grid.

[Shannon 48, Ott 02, G,T&C 06] and led to the concept of information entropy. Imagine that an experiment has N possible outcomes. If the probability of each is p_1, p_2, \dots, p_N , with normalization such that $\sum_{i=1}^N p_i = 1$, the Shannon entropy is defined as

$$S_{\text{Shannon}} = - \sum_{i=1}^N p_i \ln p_i. \quad (12.27)$$

If $p_i \equiv 0$, there is no uncertainty and $S_{\text{Shannon}} = 0$, as you might expect. If all N outcomes have equal probability, $p_i \equiv 1/N$, we obtain $S_{\text{Shannon}} = \ln N$, which diverges slowly as $N \rightarrow \infty$.

The code `Entropy.java` in Listing 12.3 computes the Shannon entropy for the the logistic map as a function of the growth parameter μ . The results (Figure 12.4 left) are seen to be quite similar to the Lyapunov exponent, again with discontinuities occurring at the bifurcations.

12.9 Unit I Quiz

1. Consider the logistic map.
 - a. Make sketches of what a graph of population x_i versus generation number i would look like for extinction and for a period-two cycle.
 - b. Describe in words and possibly a diagram the relation between the preceding two sketches and the bifurcation plot of x_i versus i .

____ -1
 ____ 0
 ____ 1



COPYRIGHT 2008, PRINCETON UNIVERSITY PRESS

EVALUATION COPY ONLY. NOT FOR USE IN COURSES.

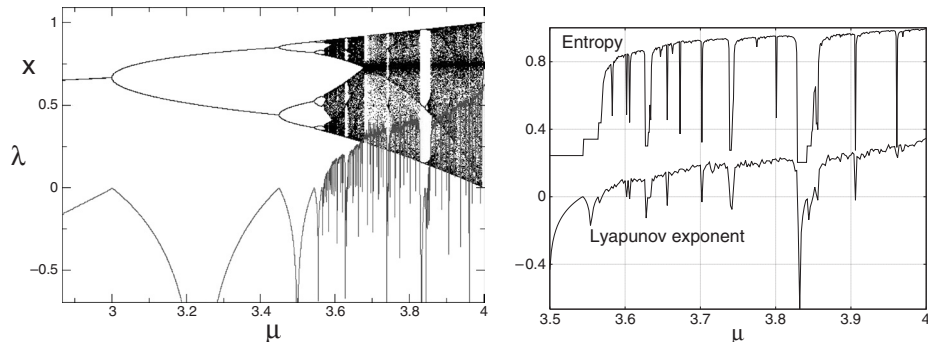


Figure 12.4 Left: Lyapunov exponent and bifurcation values for the logistic map as functions of the growth rate μ . Right: Shannon entropy (reduced by a factor of 5) and the Lyapunov coefficient for the logistic map.

2. Consider the *tent map*. Rather than compute this map, study it with just a piece of paper.
 - a. Make sketches of what a graph of population x_i versus generation number i would look like for extinction, for a period-one cycle, and for a period-two cycle.
 - b. Show that there is a single fixed point for $\mu > 1/2$ and a period-two cycle for $\mu > 1$.

```
// Entropy.java, Shannon entropy of logistic map
import java.io.*;
import java.util.*;

public class Entropy {

    public static void main(String[] argv) throws IOException, FileNotFoundException {
        PrintWriter w = new PrintWriter(new FileOutputStream("Entropy.dat"), true);
        double prob[] = new double[1001]; // Probabilities
        int nbin = 1000, nmax = 100000, j, n, ibin;
        double entropy, x, mu;
        System.out.println("Entropy output in Entropy.dat");
        for (mu = 3.5; mu <= 4.0; mu = mu + 0.001) { // Values of mu
            for (j=1; j < nbin; j++) prob[j] = 0;
            x = 0.5;
            for (n=1; n <= nmax; n++) {
                x = mu*x*(1-x); // Logistic map, Skip transients
                if (n > 30000) { ibin = (int)(x*nbin) + 1; prob[ibin] = prob[ibin] + 1; }
            }
            entropy = 0.0;
            for (ibin = 1; ibin <= nbin; ibin++) if (prob[ibin] > 0)
                entropy = entropy - (prob[ibin]/nmax)*Math.log(prob[ibin]/nmax);
            w.println(" " + mu + " " + entropy);
        }
    }
}
```

Listing 12.3 Entropy.java computes the Shannon entropy for the logistic map as a function of growth parameter μ .



COPYRIGHT 2008, PRINCETON UNIVERSITY PRESS

EVALUATION COPY ONLY. NOT FOR USE IN COURSES.

12.10 Unit II. Pendulums Become Chaotic (Continuous)



In Unit I on bugs we discovered that a simple nonlinear difference equation yields solutions that may be simple, complicated, or chaotic. Unit III will extend that model to the differential form, which also exhibits complex behaviors. Now we search for similar nonlinear, complex behaviors in the differential equation describing a realistic pendulum. Because chaotic behavior may resemble noise, it is important to be confident that the unusual behaviors arise from physics and not numerics. Before we explore the solutions, we provide some theoretical background on the use of phase space plots for revealing the beauty and simplicity underlying complicated behaviors. We also provide two chaotic pendulum applets (Figure 12.5) for assistance in understanding the new concepts. Our study is based on the description in [Rash 90], on the analytic discussion of the parametric oscillator in [L&L,M 76], and on a similar study of the vibrating pivot pendulum in [G,T&C 06].

Consider the pendulum on the left in Figure 12.5. We see a pendulum of length l driven by an external sinusoidal torque \mathbf{f} through air with a coefficient of drag α . Because there is no restriction that the angular displacement θ be small, we call this a *realistic* pendulum. Your **problem** is to describe the motion of this pendulum, first when the driving torque is turned off but the initial velocity is large enough to send the pendulum over the top, and then when the driving torque is turned on.

12.11 Chaotic Pendulum ODE

What we call a *chaotic pendulum* is just a pendulum with friction and a driving torque (Figure 12.5 left) but with no small-deflection-angle approximation. Newton's laws of rotational motion tell us that the sum of the gravitational torque $-mgl \sin \theta$, the frictional torque $-\beta \dot{\theta}$, and the external torque $\tau_0 \cos \omega t$ equals the moment of inertia of the pendulum times its angular acceleration [Rash 90]:

$$I \frac{d^2 \theta}{dt^2} = -mgl \sin \theta - \beta \frac{d\theta}{dt} + \tau_0 \cos \omega t, \quad (12.28)$$

$$\Rightarrow \frac{d^2 \theta}{dt^2} = -\omega_0^2 \sin \theta - \alpha \frac{d\theta}{dt} + f \cos \omega t, \quad (12.29)$$

$$\text{where } \omega_0 = \frac{mgl}{I}, \quad \alpha = \frac{\beta}{I}, \quad f = \frac{\tau_0}{I}. \quad (12.30)$$

Equation (12.29) is a second-order time-dependent nonlinear differential equation. Its nonlinearity arises from the $\sin \theta$, as opposed to the θ , dependence of

— — — — — 1
— — — — — 0
— — — — — 1



COPYRIGHT 2008, PRINCETON UNIVERSITY PRESS

EVALUATION COPY ONLY. NOT FOR USE IN COURSES.

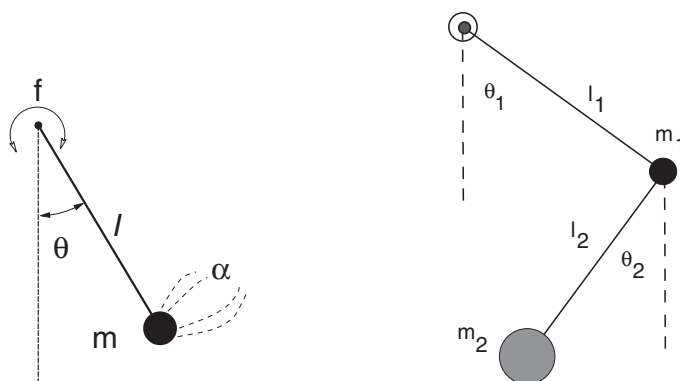


Figure 12.5 *Left:* A pendulum of length l driven through air by an external sinusoidal torque. The strength of the torque is given by f and that of air resistance by α . *Right:* A double pendulum.

the gravitational torque. The parameter ω_0 is the natural frequency of the system arising from the restoring torque, α is a measure of the strength of friction, and f is a measure of the strength of the driving torque. In our standard ODE form, $dy/dt = \mathbf{y}$ (Chapter 9, “Differential Equation Applications”), we have two simultaneous first-order equations:

$$\frac{dy^{(0)}}{dt} = y^{(1)}, \quad (12.31)$$

$$\frac{dy^{(1)}}{dt} = -\omega_0^2 \sin y^{(0)} - \alpha y^{(1)} + f \cos \omega t,$$

$$\text{where } y^{(0)} = \theta(t), \quad y^{(1)} = \frac{d\theta(t)}{dt}. \quad (12.32)$$

12.11.1 Free Pendulum Oscillations

If we ignore friction and external torques, (12.29) takes the simple form

$$\frac{d^2\theta}{dt^2} = -\omega_0^2 \sin \theta \quad (12.33)$$

If the displacements are small, we can approximate $\sin \theta$ by θ and obtain the linear equation of simple harmonic motion with frequency ω_0 :

$$\frac{d^2\theta}{dt^2} \simeq -\omega_0^2 \theta \Rightarrow \theta(t) = \theta_0 \sin(\omega_0 t + \phi). \quad (12.34)$$



In Chapter 9, “Differential Equation Applications,” we studied how nonlinearities produce anharmonic oscillations, and indeed (12.33) is another good candidate for such studies. As before, we expect solutions of (12.33) for the free realistic pendulum to be periodic, but with a frequency $\omega \simeq \omega_0$ only for small oscillations. Furthermore, because the restoring torque, $mgl \sin \theta \simeq mgl(\theta - \theta^3/3)$, is less than the $mgl\theta$ assumed in a harmonic oscillator, realistic pendulums swing slower (have longer periods) as their angular displacements are made larger.

12.11.2 Solution as Elliptic Integrals

The analytic solution to the realistic pendulum is a textbook problem [L&L,M 76, M&T 03, Schk 94], except that it is hardly a solution and hardly analytic. The “solution” is based on energy being a constant (integral) of the motion. For simplicity, we start the pendulum off at rest from its maximum displacement θ_m . Because the initial energy is all potential, we know that the total energy of the system equals its initial potential energy (Figure 12.5),

$$E = \text{PE}(0) = mgl - mgl \cos \theta_m = 2mgl \sin^2 \left(\frac{\theta_m}{2} \right). \quad (12.35)$$

Yet since $E = \text{KE} + \text{PE}$ is a constant, we can write for any value of θ

$$\begin{aligned} 2mgl \sin^2 \frac{\theta_m}{2} &= \frac{1}{2} I \left(\frac{d\theta}{dt} \right)^2 + 2mgl \sin^2 \frac{\theta}{2}, \\ \Rightarrow \frac{d\theta}{dt} &= 2\omega_0 \left[\sin^2 \frac{\theta_m}{2} - \sin^2 \frac{\theta}{2} \right]^{1/2} \Rightarrow \frac{dt}{d\theta} = \frac{T_0/\pi}{[\sin^2(\theta_m/2) - \sin^2(\theta/2)]^{1/2}}, \\ \Rightarrow \frac{T}{4} &= \frac{T_0}{4\pi} \int_0^{\theta_m} \frac{d\theta}{[\sin^2(\theta_m/2) - \sin^2(\theta/2)]^{1/2}} = \frac{T_0}{4\pi \sin \theta_m} F \left(\frac{\theta_m}{2}, \frac{\theta}{2} \right), \quad (12.36) \\ \Rightarrow T &\simeq T_0 \left[1 + \frac{1}{4} \sin^2 \frac{\theta_m}{2} + \frac{9}{64} \sin^4 \frac{\theta_m}{2} + \cdots \right], \quad (12.37) \end{aligned}$$


where we have assumed that it takes $T/4$ for the pendulum to travel from $\theta = 0$ to θ_m . The integral in (12.36) is an *elliptic integral of the first kind*. If you think of an elliptic integral as a generalization of a trigonometric function, then this is a closed-form solution; otherwise, it's an integral needing computation. The series expansion of the period (12.37) is obtained by expanding the denominator and



integrating it term by term. It tells us, for example, that an amplitude of 80° leads to a 10% slowdown of the pendulum relative to the small θ result. In contrast, we will determine the period empirically without the need for any expansions.

12.11.3 Implementation and Test: Free Pendulum

As a preliminary to the solution of the full equation (12.29), modify your rk4 program to solve (12.33) for the free oscillations of a realistic pendulum.

1. Start your pendulum at $\theta = 0$ with $\dot{\theta}(0) \neq 0$. Gradually increase $\dot{\theta}(0)$ to increase the importance of nonlinear effects.
2. Test your program for the linear case ($\sin \theta \rightarrow \theta$) and verify that
 - a. your solution is harmonic with frequency $\omega_0 = 2\pi/T_0$, and
 - b. the frequency of oscillation is independent of the amplitude.
3. Devise an algorithm to determine the period T of the oscillation by counting the time it takes for three successive passes of the amplitude through $\theta = 0$. (You need *three* passes because a general oscillation may not be symmetric about the origin.) Test your algorithm for simple harmonic motion where you know T_0 .
4. For the realistic pendulum, observe the change in period as a function of increasing initial energy or displacement. Plot your observations along with (12.37).
5. Verify that as the initial KE approaches $2mgl$, the motion remains oscillatory but not harmonic (Figure 12.8).
6. At $E = 2mgl$ (the *separatrix*), the motion changes from oscillatory to rotational (“over the top” or “running”). See how close you can get to the separatrix and to its infinite period.
7.  Use the applet **HearData** (Figure 12.6) to convert your different oscillations to sound and hear the difference between harmonic motion (boring) and anharmonic motion containing overtones (interesting).

12.12 Visualization: Phase Space Orbits

The conventional solution to an equation of motion is the position $x(t)$ and the velocity $v(t)$ as functions of time. Often behaviors that appear complicated as functions of time appear simpler when viewed in an abstract space called *phase space*, where the ordinate is the velocity $v(t)$ and the abscissa is the position $x(t)$ (Figure 12.7). As we see from the phase space figures, the solutions form geometric objects that are easy to recognize. (We provide two applets on the CD, **Pend1** and **Pend2**, to help the reader make the connections between phase space shapes and the corresponding physical motion.)



COPYRIGHT 2008, PRINCETON UNIVERSITY PRESS

EVALUATION COPY ONLY. NOT FOR USE IN COURSES.

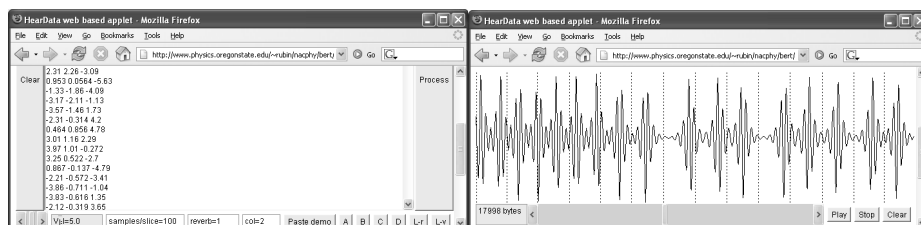


Figure 12.6 The data screen (left) and output screen (right) of the applet **HearData**, on the CD. Columns of $(t_i, x(t_i))$ data are pasted into the data window, processed into the graph in the output window, and then converted to sound that is played by Java.

The position and velocity of a free harmonic oscillator are given by the trigonometric functions

$$x(t) = A \sin(\omega t), \quad v(t) = \frac{dx}{dt} = \omega A \cos(\omega t). \quad (12.38)$$

When substituted into the total energy, we obtain two important results:

$$E = \text{KE} + \text{PE} = \left(\frac{1}{2}m\right) v^2 + \left(\frac{1}{2}\omega^2 m^2\right) x^2 \quad (12.39)$$

$$= \frac{\omega^2 m^2 A^2}{2m} \cos^2(\omega t) + \frac{1}{2}\omega^2 m^2 A^2 \sin^2(\omega t) = \frac{1}{2}m\omega^2 A^2. \quad (12.40)$$

The first equation, being that of an ellipse, proves that the harmonic oscillator follows closed elliptical orbits in phase space, with the size of the ellipse increasing with the system's energy. The second equation proves that the total energy is a constant of the motion. Different initial conditions having the same energy start at different places on the same ellipse and transverse the same orbits.

In Figures 12.7–12.10 we show various phase space structures. *Study these figures and their captions* and note the following:

- The orbits of anharmonic oscillations will still be ellipselike but with angular corners that become more distinct with increasing nonlinearity.
- Closed trajectories describe periodic oscillations [the same (x, v) occur again and again], with clockwise motion.
- Open orbits correspond to nonperiodic or “running” motion (a pendulum rotating like a propeller).
- Regions of space where the potential is repulsive lead to open trajectories in phase space (Figure 12.7 left).



COPYRIGHT 2008, PRINCETON UNIVERSITY PRESS

EVALUATION COPY ONLY. NOT FOR USE IN COURSES.

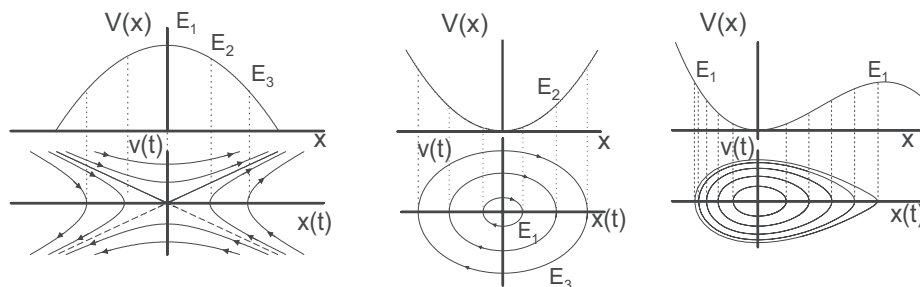


Figure 12.7 Three potentials and their characteristic behaviors in phase space. The different orbits correspond to different energies, as indicated by the limits within the potentials (dashed lines). Notice the absence of trajectories in regions forbidden by energy conservation. *Left:* A repulsive potential leads to open orbits in phase space characteristic of nonperiodic motion. The phase space trajectories cross at the hyperbolic point in the middle, an unstable equilibrium point. *Middle:* The harmonic oscillator leads to symmetric ellipses in phase space; the closed orbits indicate periodic behavior, and the symmetric trajectories indicate a symmetric potential. *Right:* A nonharmonic oscillator. Notice that the ellipselike trajectories neither are ellipses nor are symmetric with respect to the $v(t)$ axis.

- As seen in Figure 12.8 left, the separatrix corresponds to the trajectory in phase space that separates open and closed orbits. Motion on the separatrix is indeterminant, as the pendulum may balance at the maxima of $V(\theta)$.
- Friction may cause the energy to decrease with time and the phase space orbit to spiral into a *fixed point*.
- For certain parameters, a closed *limit cycle* occurs in which the energy pumped in by the external torque exactly balances that lost by friction (Figure 12.8 right).
- Because solutions for different initial conditions are unique, different orbits do not cross. Nonetheless, open orbits join at points of unstable equilibrium (*hyperbolic points* in Figure 12.7 left) where an indeterminacy exists. **I**

12.12.1 Chaos in Phase Space

It is easy to solve the nonlinear ODE (12.31) on the computer using our usual techniques. However, it is not so easy to understand the solutions because they are so rich in complexity. The solutions are easier to understand in phase space, particularly if you learn to recognize some characteristic structures there. Actually, there are a number of “tools” that can be used to decide if a system is chaotic in contrast to just complex. Geometric structures in phase space is one of them,

— -1
— 0
— 1



COPYRIGHT 2008, PRINCETON UNIVERSITY PRESS

EVALUATION COPY ONLY. NOT FOR USE IN COURSES.

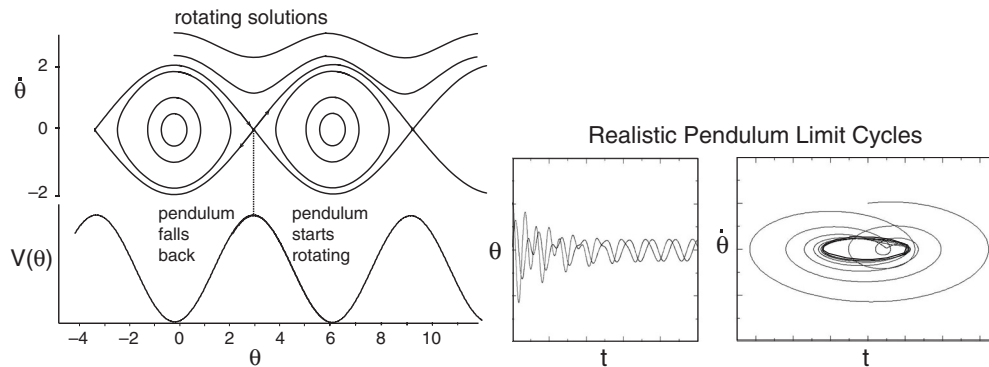


Figure 12.8 Left: Phase space trajectories for a plane (i.e. 2-D) pendulum including “over the top” or rotating solutions. The trajectories are symmetric with respect to vertical and horizontal reflections through the origin. At the bottom of the figure is shown the corresponding θ dependence of the potential. Right: Position *versus* time for two initial conditions of a chaotic pendulum that end up with the same limit cycle, and the corresponding phase space orbits. (Courtesy of W. Hager.)

and determination of the Lyapunov coefficient (discussed in §12.8) is another. Both signal the simplicity lying within the complexity.

What may be surprising is that even though the ellipselike figures in phase space were observed originally for free systems with no friction and no driving torque, similar structures continue to exist for driven systems with friction. The actual trajectories may not remain on a single structure for all times, but they are *attracted* to them and return to them often. In contrast to periodic motion, which corresponds to closed figures in phase space, random motion appears as a diffuse cloud filling an entire energetically accessible region. Complex or chaotic motion falls someplace in between (Figure 12.9 middle). If viewed for long times and for many initial conditions, chaotic trajectories (flows) through phase space, while resembling the familiar geometric figures, they may contain dark or diffuse *bands* in places rather than single lines. The continuity of trajectories within bands means that a continuum of solutions is possible and that the system flows continuously among the different trajectories forming the band. The transitions among solutions cause the coordinate space solutions to appear chaotic and are what makes them hypersensitive to the initial conditions (the slightest change in which causes the system to flow to nearby trajectories).

Pick out the following phase space structures in your simulations.

Limit cycles: When a chaotic pendulum is driven by a not-too-large driving torque, it is possible to pick the magnitude for this torque such that after the initial transients die off, the average energy put into the system during one period exactly balances the average energy dissipated by friction during that

— -1
— 0
— 1



COPYRIGHT 2008, PRINCETON UNIVERSITY PRESS

EVALUATION COPY ONLY. NOT FOR USE IN COURSES.

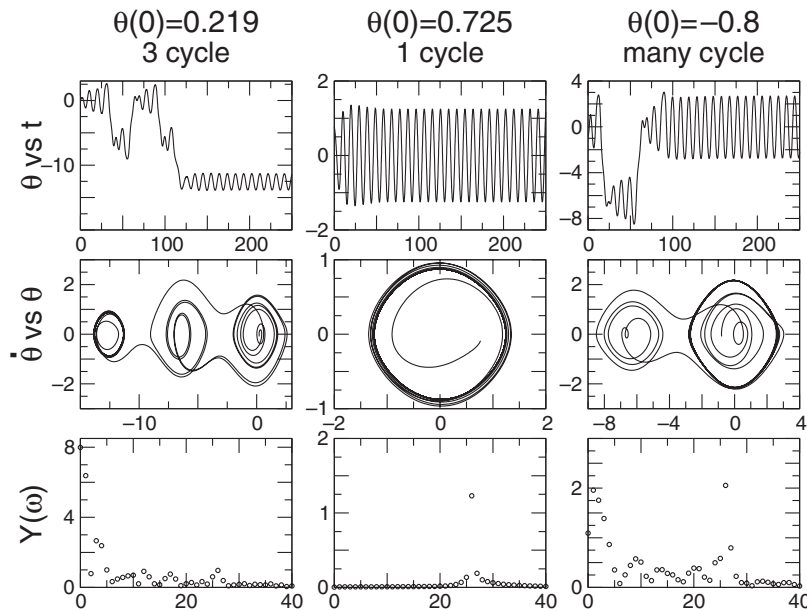


Figure 12.9 Position and phase space plots for a chaotic pendulum with $\omega_0 = 1$, $\alpha = 0.2$, $f = 0.52$, and $\omega = 0.666$. The rightmost initial condition displays more of the broadband Fourier spectrum characteristic of chaos. (Examples of chaotic behavior can be seen in Figure 12.10.)

period (Figure 12.8 right):

$$\langle f \cos \omega t \rangle = \left\langle \alpha \frac{d\theta}{dt} \right\rangle = \left\langle \alpha \frac{d\theta(0)}{dt} \cos \omega t \right\rangle \Rightarrow f = \alpha \frac{d\theta(0)}{dt}. \quad (12.41)$$

This leads to *limit cycles* that appear as closed ellipselike figures, yet the solution may be unstable and make sporadic jumps between limit cycles.

Predictable attractors: Well-defined, fairly simple periodic behaviors that are not particularly sensitive to the initial conditions. These are orbits, such as fixed points and limit cycles, into which the system settles or returns to often. If your location in phase space is near a predictable attractor, ensuing times will bring you to it.

Strange attractors: Well-defined, yet complicated, semiperiodic behaviors that appear to be uncorrelated with the motion at an earlier time. They are distinguished from predictable attractors by being fractal (Chapter 13, “Fractals & Statistical Growth”) chaotic, and highly sensitive to the initial conditions [J&S 98]. Even after millions of oscillations, the motion remains *attracted* to them.



COPYRIGHT 2008, PRINCETON UNIVERSITY PRESS

EVALUATION COPY ONLY. NOT FOR USE IN COURSES.

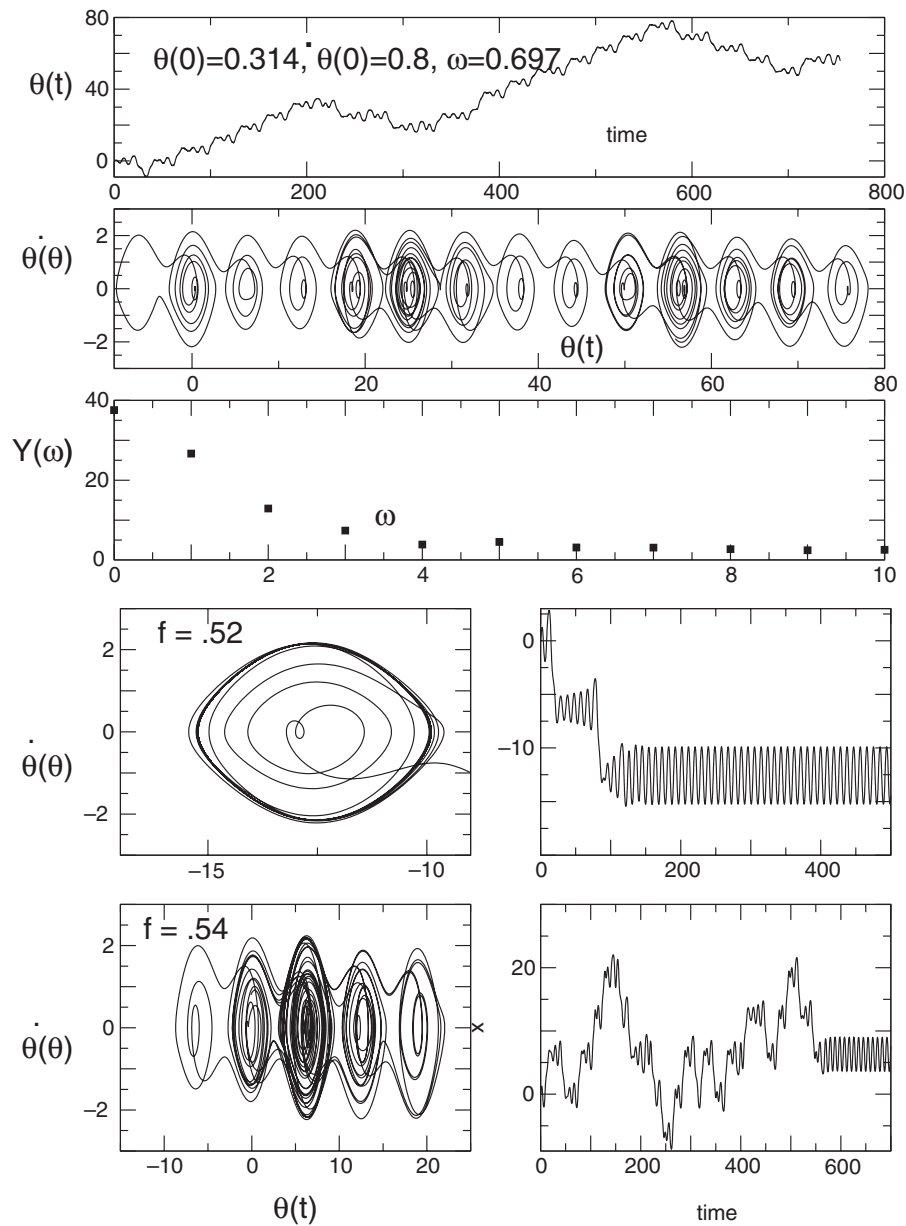


Figure 12.10 Some examples of complicated behaviors of a realistic pendulum. In the top three rows sequentially we see $\theta(t)$ behaviors, a phase space diagram containing regular patterns with dark bands, and a broad Fourier spectrum. These features are characteristic of chaos. In the bottom two rows we see how the behavior changes abruptly after a slight change in the magnitude of the force and that for $f=0.54$ there occur the characteristic broad bands of chaos.



COPYRIGHT 2008, PRINCETON UNIVERSITY PRESS

EVALUATION COPY ONLY. NOT FOR USE IN COURSES.

Chaotic paths: Regions of phase space that appear as filled-in bands rather than lines. Continuity within the bands implies complicated behaviors, yet still with simple underlying structure.

Mode locking: When the magnitude f of the driving torque is larger than that for a limit cycle (12.41), the driving torque can overpower the natural oscillations, resulting in a steady-state motion at the frequency of the driver. This is called *mode locking*. While mode locking can occur for linear or nonlinear systems, for nonlinear systems the driving torque may lock onto the system by exciting its overtones, leading to a rational relation between the driving frequency and the natural frequency:

$$\frac{\omega}{\omega_0} = \frac{n}{m}, \quad n, m = \text{integers.} \quad (12.42)$$

Butterfly effects: One of the classic quips about the hypersensitivity of chaotic systems to the initial conditions is that the weather pattern in North America is hard to predict well because it is sensitive to the flapping of butterfly wings in South America. Although this appears to be counterintuitive because we know that systems with essentially identical initial conditions should behave the same, eventually the systems diverge. The applet `pend2` (Figure 12.11 bottom) lets you compare two simulations of nearly identical initial conditions. As seen on the right in Figure 12.11, the initial conditions for both pendulums differ by only 1 part in 917, and so the initial paths in phase space are the same. Nonetheless, at just the time shown here, the pendulums balance in the vertical position, and then one falls before the other, leading to differing oscillations and differing phase space plots from this time onward.

12.12.2 Assessment in Phase Space

The challenge in understanding simulations of the chaotic pendulum (12.31) is that the 4-D parameter space $(\omega_0, \alpha, f, \omega)$ is so immense that only sections of it can be studied systematically. We expect that sweeping through driving frequency ω should show resonances and beating; sweeping through the frictional force α should show underdamping, critical damping, and overdamping; and sweeping through the driving torque f should show mode locking (for the right values of ω). All these behaviors can be found in the solution of your differential equation, yet they are mixed together in complex ways.

In this assessment you should try to reproduce the behaviors shown in the phase space diagrams in Figure 12.9 and in the applets in Figure 12.11. *Beware:* Because the system is chaotic, you should expect that your results will be sensitive to the exact values of the initial conditions and to the details of your integration routine. We suggest that you experiment; start with the parameter values we used to produce our plots and then observe the effects of making *very small* changes in parameters

— -1
— 0
— 1



COPYRIGHT 2008, PRINCETON UNIVERSITY PRESS

EVALUATION COPY ONLY. NOT FOR USE IN COURSES.

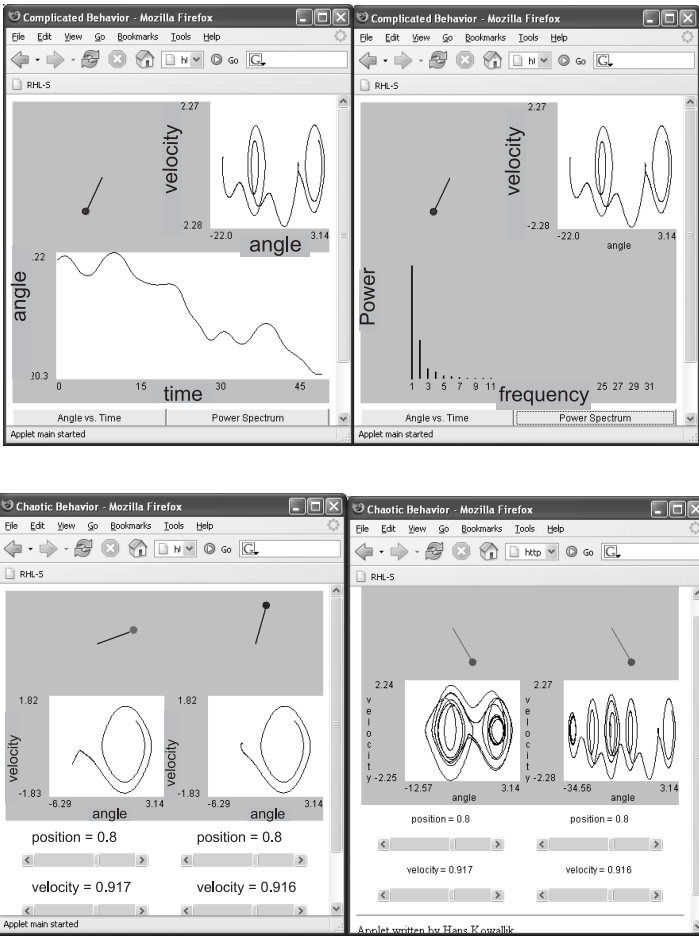


Figure 12.11 Top row: Output from the applet `Pend1` producing an animation of a chaotic pendulum, along with the corresponding position *versus* time and phase space plots. Right: the resulting Fourier spectrum produced by `Pend1`, Bottom row: output from the applet `Pend2` producing an animation of two chaotic pendula, along with the corresponding phase space plots, and the final output with limit cycles (dark bands).

until you obtain different modes of behavior. Consequently, an inability to reproduce our results for the parameter values does not necessarily imply that something is “wrong.”

1. Take your solution to the realistic pendulum and include friction, making α an input parameter. Run it for a variety of initial conditions, including over-the-top ones. Since no energy is fed to the system, you should see spirals.

2. Next, verify that with no friction, but with a very small driving torque, you obtain a perturbed ellipse in phase space.
3. Set the driving torque's frequency to be close to the natural frequency ω_0 of the pendulum and search for beats (Figure 12.6 right). Note that you may need to adjust the magnitude and phase of the driving torque to avoid an "impedance mismatch" between the pendulum and driver.
4. Finally, scan the frequency ω of the driving torque and search for nonlinear resonance (it looks like beating).
5. **Explore chaos:** Start off with the initial conditions we used in Figure 12.9,

$$(x_0, v_0) = (-0.0885, 0.8), \quad (-0.0883, 0.8), \quad (-0.0888, 0.8).$$

To save time and storage, you may want to use a larger time step for plotting than the one used to solve the differential equations.

6. Indicate which parts of the phase space plots correspond to transients. (The applets on the CD may help you with this, especially if you watch the phase space features being built up in time.)
7. Ensure that you have found:
 - a. a period-3 limit cycle where the pendulum jumps between three major orbits in phase space,
 - b. a running solution where the pendulum keeps going over the top,
 - c. chaotic motion in which some paths in the phase space appear as bands.
8. Look for the "butterfly effect" (Figure 12.11 bottom). Start two pendulums off with identical positions but with velocities that differ by 1 part in 1000. Notice that the initial motions are essentially identical but that at some later time the motions diverge.

12.13 Exploration: Bifurcations of Chaotic Pendulums

We have seen that a chaotic system contains a number of dominant frequencies and that the system tends to "jump" from one to another. This means that the dominant frequencies occur sequentially, in contrast to linear systems where they occur simultaneously. We now want to explore this jumping as a computer experiment. If we sample the instantaneous angular velocity $\dot{\theta} = d\theta/dt$ of our chaotic simulation at various instances in time, we should obtain a series of values for the frequency, with the major Fourier components occurring more often than others.³ These are the frequencies to which the system is *attracted*. That being the case, if we make a scatterplot of the sampled $\dot{\theta}$ s for many times at one particular value of the driving force and then change the magnitude of the driving force slightly and sample the frequencies again, the resulting plot may show distinctive patterns of frequencies. That a bifurcation diagram similar to the one for bug populations results is one of the mysteries of life.

³ We refer to this angular velocity as $\dot{\theta}$ since we have already used ω for the frequency of the driver and ω_0 for the natural frequency.



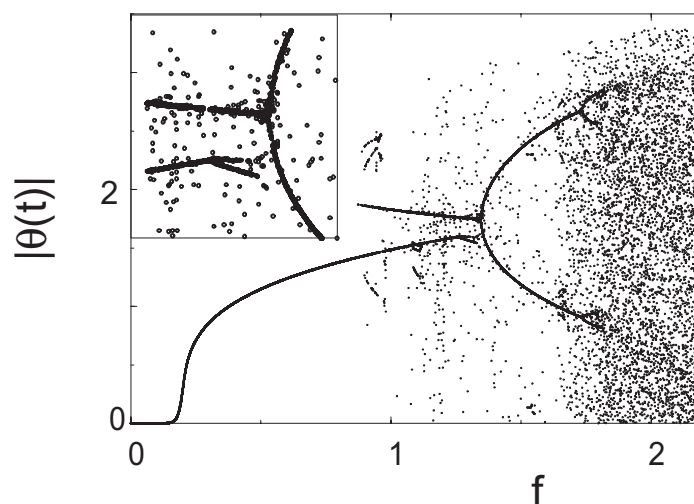


Figure 12.12 A bifurcation diagram for the damped pendulum with a vibrating pivot (see also the similar diagram for a double pendulum, Figure 12.14). The ordinate is $|d\theta/dt|$, the absolute value of the instantaneous angular velocity at the beginning of the period of the driver, and the abscissa is the magnitude of the driving force f . Note that the heavy line results from the overlapping of points, not from connecting the points (see enlargement in the inset).

In the scatterplot in Figure 12.12, we sample $\dot{\theta}$ for the motion of a chaotic pendulum with a vibrating pivot point (in contrast to our usual vibrating external torque). This pendulum is similar to our chaotic one (12.29), but with the driving force depending on $\sin \theta$:

$$\frac{d^2\theta}{dt^2} = -\alpha \frac{d\theta}{dt} - (\omega_0^2 + f \cos \omega t) \sin \theta. \quad (12.43)$$

Essentially, the acceleration of the pivot is equivalent to a sinusoidal variation of g or ω_0^2 . Analytic [L&L,M 76, §25–30] and numeric [DeJ 92, G,T&C 06] studies of this system exist. To obtain the bifurcation diagram in Figure 12.12:

1. Use the initial conditions $\theta(0) = 1$ and $\dot{\theta}(0) = 1$.
2. Set $\alpha = 0.1$, $\omega_0 = 1$, and $\omega = 2$, and vary $0 \leq f \leq 2.25$.
3. For each value of f , wait 150 periods of the driver before sampling to permit transients to die off. Sample $\dot{\theta}$ for 150 times at the instant the driving force passes through zero.
4. Plot the 150 values of $|\dot{\theta}|$ versus f .



COPYRIGHT 2008, PRINCETON UNIVERSITY PRESS

EVALUATION COPY ONLY. NOT FOR USE IN COURSES.

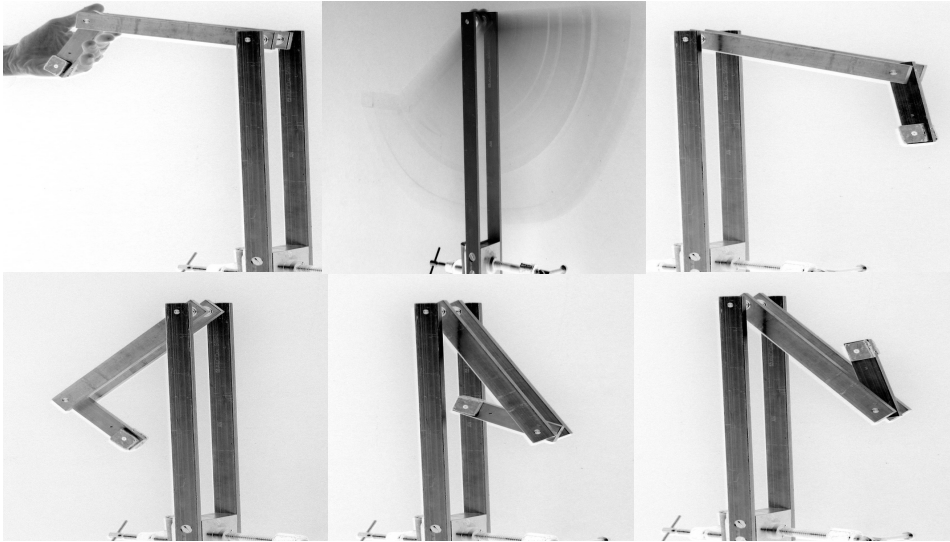


Figure 12.13 Photographs of a double pendulum built by a student in the OSU Physics Department. The longer pendulum consists of two separated shafts so that the shorter one can rotate through it. Both pendula can go over the top. We see the pendulum released from rest and then moving quickly. The flash photography stops the motion in various stages. (Photograph, R. Landau.)

12.14 Alternative Problem: The Double Pendulum

For those of you who have already studied a chaotic pendulum, an alternative is to study a double pendulum without any small-angle approximation (Figure 12.5 right and Fig. 12.13, and animation DoublePend.mpg on the CD). A double pendulum has a second pendulum connected to the first, and because each pendulum acts as a driving force for the other, we need not include an external driving torque to produce a chaotic system (there are enough degrees of freedom without it).

The equations of motions for the double pendulum are derived most directly from the Lagrangian formulation of mechanics. The Lagrangian is fairly simple but has the θ_1 and θ_2 motions innately coupled:

$$L = \text{KE} - \text{PE} = \frac{1}{2}(m_1 + m_2)l_1^2\dot{\theta}_1^2 + \frac{1}{2}m_2l_2^2\dot{\theta}_2^2 + m_2l_1l_2\dot{\theta}_1\dot{\theta}_2\cos(\theta_1 - \theta_2) + (m_1 + m_2)gl_1\cos\theta_1 + m_2gl_2\cos\theta_2. \quad (12.44)$$



COPYRIGHT 2008, PRINCETON UNIVERSITY PRESS

EVALUATION COPY ONLY. NOT FOR USE IN COURSES.

— 1
— 0
— 1

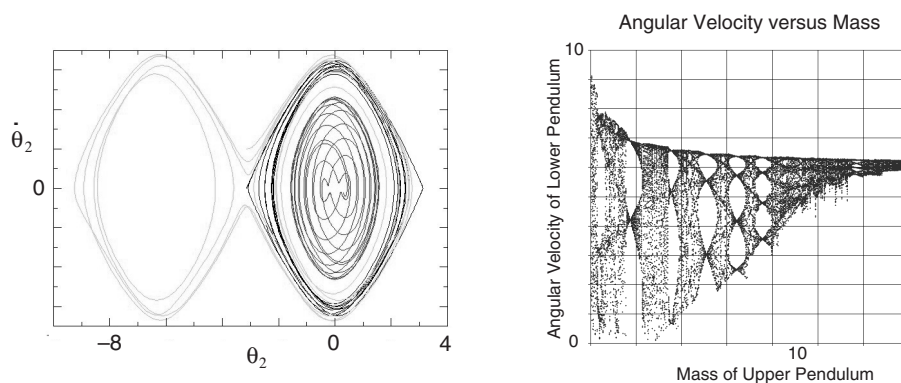


Figure 12.14 *Left:* Phase space trajectories for a double pendulum with $m_1 = 10m_2$, showing two dominant attractors. *Right:* A bifurcation diagram for the double pendulum displaying the instantaneous velocity of the lower pendulum as a function of the mass of the upper pendulum. (Both plots are courtesy of J. Danielson.)

The resulting dynamic equations couple the θ_1 and θ_2 motions:

$$(m_1 + m_2)l_1\ddot{\theta}_1 + m_2l_2\ddot{\theta}_2 \cos(\theta_1 - \theta_2) + m_2l_2\dot{\theta}_2^2 \sin(\theta_1 - \theta_2) + g(m_1 + m_2) \sin \theta_1 = 0, \quad (12.45)$$

$$m_2l_2\ddot{\theta}_2 + m_2l_1\ddot{\theta}_1 \cos(\theta_1 - \theta_2) - m_2l_1\dot{\theta}_1^2 \sin(\theta_1 - \theta_2) + mg \sin \theta_2 = 0. \quad (12.46)$$

Usually textbooks approximate these equations for small oscillations, which diminish the effects of the coupling. “Slow” and “fast” modes then result for in-phase and antiphase oscillations, respectively, that look much like regular harmonic motions. What’s more interesting is the motion that results without any small-angle restrictions, particularly when the pendulums have enough initial energy to go over the top (Figure 12.13). On the left in Figure 12.14 we see several phase space plots for the lower pendulum with $m_1 = 10m_2$. When given enough initial kinetic energy to go over the top, the trajectories are seen to flow between two major attractors as energy is transferred back and forth to the upper pendulum.

On the right in Figure 12.14 is a bifurcation diagram for the double pendulum. This was created by sampling and plotting the instantaneous angular velocity $\dot{\theta}_2$ of the lower pendulum at 70 times as the pendulum passed through its equilibrium position. The mass of the upper pendulum (a convenient parameter) was then changed, and the process repeated. The resulting structure is fractal and indicates bifurcations in the number of dominant frequencies in the motion. A plot of the Fourier or wavelet spectrum as a function of mass is expected to show similar characteristic frequencies.



COPYRIGHT 2008, PRINCETON UNIVERSITY PRESS

EVALUATION COPY ONLY. NOT FOR USE IN COURSES.

12.15 Assessment: Fourier/Wavelet Analysis of Chaos

We have seen that a realistic pendulum experiences a restoring torque, $\tau_g \propto \sin \theta \simeq \theta - \theta^3/3! + \theta^5/5! + \dots$, that contains nonlinear terms that lead to nonharmonic behavior. In addition, when a realistic pendulum is driven by an external sinusoidal torque, the pendulum may mode-lock with the driver and so oscillate at a frequency that is rationally related to the driver's. Consequently, the behavior of the realistic pendulum is expected to be a combination of various periodic behaviors, with discrete jumps between modes.

In this assessment you should determine the Fourier components present in the pendulum's complicated and chaotic behaviors. You should show that a three-cycle structure, for example, contains three major Fourier components, while a five-cycle structure has five. You should also notice that when the pendulum goes over the top, its spectrum contains a steady-state (DC) component.

1. Dust off your program for analyzing a $y(t)$ into Fourier components. Alternatively, you may use a Fourier analysis tool contained in your graphics program or system library (e.g., Grace and OpenDX).
2. Apply your analyzer to the solution of the chaotic pendulum for the cases where there are one-, three-, and five-cycle structures in phase space. Deduce the major frequencies contained in these structures.
3. Compare your results with the output of the Pend1 applet (Figure 12.11 top).
4. Try to deduce a relation among the Fourier components, the natural frequency ω_0 , and the driving frequency ω .
5. A classic signal of chaos is a broadband, although not necessarily flat, Fourier spectrum. Examine your system for parameters that give chaotic behavior and verify this statement.

Wavelet Exploration: We saw in Chapter 11, "Wavelet Analysis & Data Compression", that a wavelet expansion is more appropriate than a Fourier expansion for a signal containing components that occur for finite periods of time. Because chaotic oscillations are just such signals, repeat the Fourier analysis of this section using wavelets instead of sines and cosines. Can you discern the temporal sequence of the various components?

12.16 Exploration: Another Type of Phase Space Plot

Imagine that you have measured the displacement of some system as a function of time. Your measurements appear to indicate characteristic nonlinear behaviors, and you would like to check this by making a phase space plot but without going to the trouble of measuring the conjugate momenta to plot *versus* displacement. Amazingly enough, one may also plot $x(t + \tau)$ *versus* $x(t)$ as a function of time to obtain a phase space plot [Abar 93]. Here τ is a *lag time* and should be chosen as

— -1
— 0
— 1



COPYRIGHT 2008, PRINCETON UNIVERSITY PRESS

EVALUATION COPY ONLY. NOT FOR USE IN COURSES.

$$v(t) = \frac{dx(t)}{dt} \simeq \frac{x(t+\tau) - x(t)}{\tau}. \quad (12.47)$$

Exercise: Create a phase space plot from the output of your chaotic pendulum by plotting $\theta(t + \tau)$ versus $\theta(t)$ for a large range of t values. Explore how the graphs change for different values of the lag time τ . Compare your results to the conventional phase space plots you obtained previously.

1. The nonlinear behavior in once-common objects such as vacuum tubes and metronomes is described by the **van der Pool equation**,

The behavior predicted for these systems is *self-limiting* because the equation contains a limit cycle that is also a predictable attractor. You can think of (12.48) as describing an oscillator with x -dependent damping (the μ term). If $x > x_0$, friction slows the system down; if $x < x_0$, friction speeds the system up. Orbits internal to the limit cycle spiral out until they reach the limit cycle; orbits external to it spiral in.

- $$\frac{d^2\theta}{dt^2} - \frac{1}{2}\theta(1-\theta^2) = -\alpha \frac{d\theta}{dt} + f \cos \omega t. \quad (12.49)$$

3. **Lorenz attractor:** In 1962 Lorenz [Tab 89] was looking for a simple model for weather prediction and simplified the heat transport equations to

The solution of these simultaneous first-order nonlinear equations gave the complicated behavior that has led to the modern interest in chaos (after considerable doubt regarding the reliability of the numerical solutions).

4. **A 3-D computer fly:** Make $x + y$, $x + z$, and $y + z$ plots of the equations

$$x = \sin ay - z \cos bx, \quad y = z \sin cx - \cos dy, \quad z = e \sin x. \quad (12.51)$$

Here the parameter e controls the degree of apparent randomness.

5. **Hénon–Heiles potential:** The potential and Hamiltonian

$$V(x, y) = \frac{1}{2}x^2 + \frac{1}{2}y^2 + x^2y - \frac{1}{3}y^3, \quad H = \frac{1}{2}p_x^2 + \frac{1}{2}p_y^2 + V(x, y), \quad (12.52)$$

are used to describe three interacting astronomical objects. The potential binds the objects near the origin but releases them if they move far out. The equations of motion follow from the Hamiltonian equations:

$$\frac{dp_x}{dt} = -x - 2xy, \quad \frac{dp_y}{dt} = -y - x^2 + y^2, \quad \frac{dx}{dt} = p_x, \quad \frac{dy}{dt} = p_y.$$

- Numerically solve for the position $[x(t), y(t)]$ for a particle in the Hénon–Heiles potential.
- Plot $[x(t), y(t)]$ for a number of initial conditions. Check that the initial condition $E < \frac{1}{6}$ leads to a bounded orbit.
- Produce a Poincaré section in the (y, p_y) plane by plotting (y, p_y) each time an orbit passes through $x = 0$.

12.18 Unit III. Coupled Predator–Prey Models

In Unit I we saw complicated behavior arising from a model of bug population dynamics in which we imposed a maximum population. We described that system with a discrete logistic map. In Unit II we saw complex behaviors arising from differential equations and learned how to use phase space plots to understand them. In this unit we study the differential equation model describing predator–prey population dynamics proposed by the American physical chemist Lotka [Lot 25] and the Italian mathematician Volterra [Volt 26]. Differential equations are easy to solve numerically and should be a good approximation if populations are large. However, there are equivalent discrete map versions of the model as well. Though simple, versions of these equations are used to model biological systems and neural networks.

Problem: Is it possible to use a small number of predators to control a population of pests so that the number of pests remains approximately constant? Include in your considerations the interaction between the populations as well as the competition for food and predation time.

— 1
— 0
— 1



COPYRIGHT 2008, PRINCETON UNIVERSITY PRESS

EVALUATION COPY ONLY. NOT FOR USE IN COURSES.